Title: Active *E. coli* heteromeric acetyl-CoA carboxylase forms polymorphic helical tubular filaments

Authors: Xueyong Xu[1†], Amanda Silva de Sousa[2,3†], Trevor J. Boram[3], Wen Jiang[1]* and Jeremy R. Lohman[2,3]*

Affiliations:

[1]Department of Biological Sciences, Purdue University; West Lafayette, IN 47907 USA.

[2] Department of Biochemistry and Molecular Biology, Michigan State University; East Lansing, MI 48824 USA.

[3] Department of Biochemistry, Purdue University; West Lafayette, IN 47907 USA.

*Corresponding authors. Email: jlohman@msu.edu, jiang12@purdue.edu

[†] These authors contributed equally to this work

Abstract: The *Escherichia coli* heteromeric acetyl-CoA carboxylase (ACC) has four subunits assumed to form an elusive catalytic complex and are involved in allosteric and transcriptional regulation. The *E. coli* ACC represents almost all ACCs from pathogenic bacteria making it a key antibiotic development target to fight growing antibiotic resistance. Furthermore, it is a model for cyanobacterial and plant plastid ACCs as biofuel engineering targets. Here we report the catalytic *E. coli* ACC complex surprisingly forms tubes rather than dispersed particles. The cryo-EM structure reveals key protein-protein interactions underpinning efficient catalysis and how transcriptional regulatory roles are masked during catalysis. Discovering the protein-protein interaction interfaces that facilitate catalysis, allosteric and transcriptional regulation provides new routes to engineering catalytic activity and new targets for drug discovery.

One-Sentence Summary: Bacterial heteromeric acetyl-CoA carboxylase forms tubes to promote efficient catalysis and mask transcriptional regulation.

Main Text:

As the first committed step in fatty acids biosynthesis, acetyl-CoA carboxylases (ACCs) are highly regulated. In the majority of prokaryotes such as *Escherichia coli*, ACCs are heteromeric consisting of four proteins forming three subunits.[1] End-products of fatty acid biosynthesis allosterically feedback regulate heteromeric ACCs, although the site of action is unknown.[2-4] Some *E. coli* ACC subunits regulate their own transcription,[5,6] and one ACC subunit is known to interact with nitrogen assimilation regulatory protein GlnB,[7-9] revealing broader transcriptional regulatory roles. However, the most important mode of prokaryotic heteromeric ACC regulation is through the formation of a distinct complex which is yet to be isolated and structurally characterized.[10] Most plants have plastid associated heteromeric ACCs, for which the *E. coli* ACC is a model system.[11] The heteromeric *E. coli* ACC is necessary for growth and conserved in most bacterial pathogens, making them validated and promising antibiotic development targets.[12] Thus, an *E. coli* ACC complex structure will provide knowledge essential for both antibiotic development and biofuel engineering.

Early studies reported that *E. coli*-like heteromeric ACC complexes readily disassociate upon cell lysis, which prevented experimentation on the native complex.[10,13-15] Nevertheless, the three dissociated ACC subunits can be assayed individually or reconstituted into a complete system. In the first catalytic step, a 100 kDa homodimeric biotin carboxylase subunit (BC, AccC) uses ATP and bicarbonate to generate carboxy-biotin linked to a 17 kDa biotin-carboxy carrier protein (BCCP, AccB)(Fig. 1).[16-21] In the second step, the carboxy-BCCP translocates to a 136 kDa heterodimeric carboxyltransferase subunit (CT, AccA/AccD), where the carboxy group is transferred to acetyl-CoA to generate malonyl-CoA.[22] In vitro studies demonstrated that protein:protein interactions (PPI) within the reconstituted ACC complex alter reaction kinetics and prevent the reverse reaction, establishing a regulatory role for complex formation.[15,23,24] While crystal structures of the individual subunits are known, some disordered regions could not be modeled and are likely responsible for the PPIs (Fig. 1A).

Due to the importance of prokaryotic ACCs as the rate limiting step of fatty acid biosynthesis,[25] we desired a picture of how the PPIs in the ACC complex regulates catalytic activity of the subunits. Here we report single-particle cryo-EM structures of active *E. coli* ACC, revealing the system surprisingly forms large polymorphic helical tubular filaments. Tube formation 1) ensures the BC and CT dimeric nature is satisfied in the complex, 2) places the active sites in close proximity and 3) obscures parts of the subunits involved in transcriptional regulation.

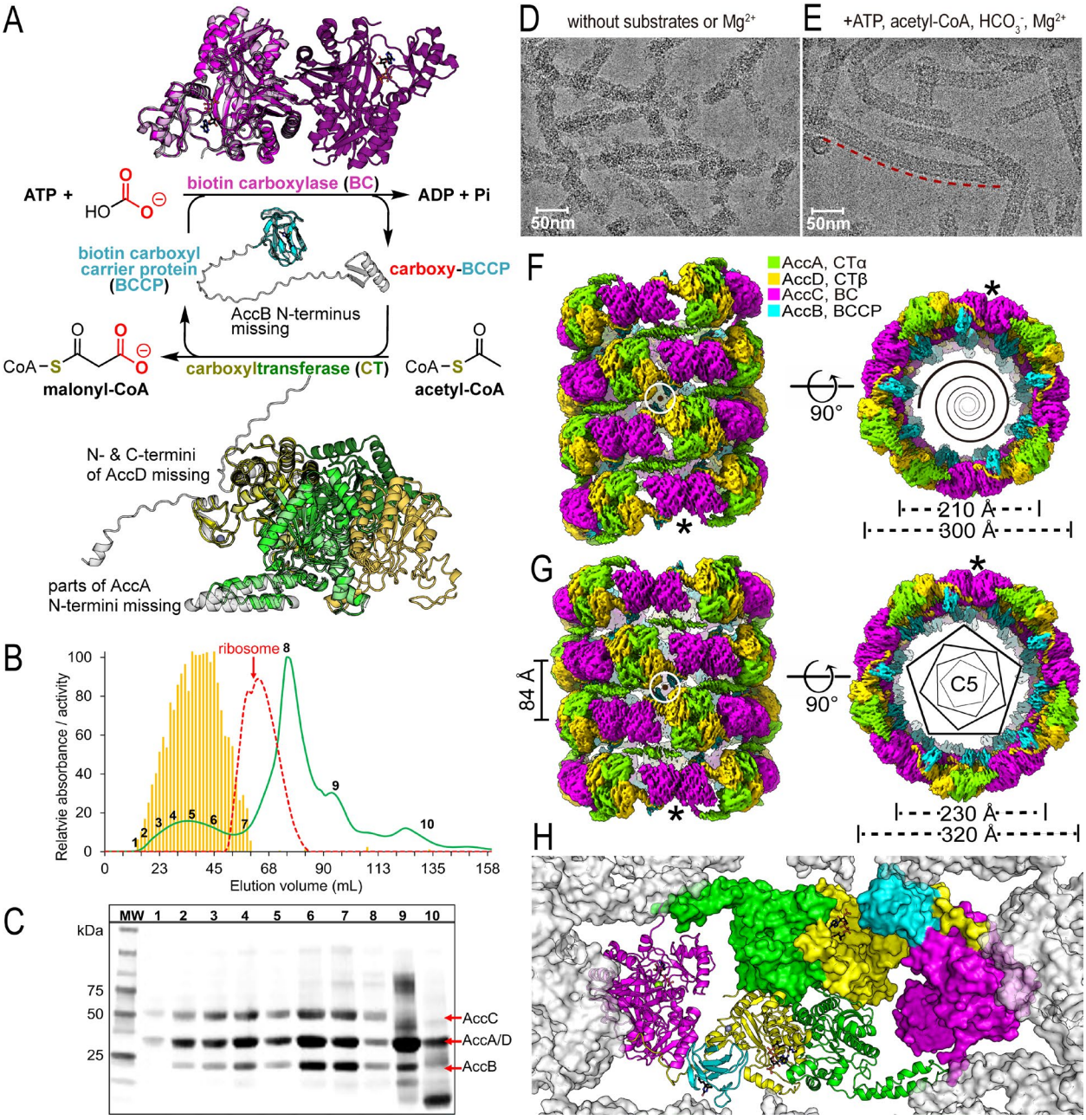

Fig. 1. Catalytic activity, purification and cryo-EM structures of *E. coli* ACC. (**A**) Catalytic activity and structures of isolated *E. coli* ACC subunits. Two distinct catalytic activities of the ACC system are shown in the center. Previous crystal structures of AccC (PDB 1DV2) are colored magenta, AccB (PDB 1BDO) colored cyan and AccA:AccD system (PDB 2F9Y) colored green/yellow, respectively and their respective AlphaFold models (shown in light gray). Colors are carried through subsequent figures. The N-termini of AccA/B/D and C-termini of AccD are predicted in the AlphaFold models but missing in published crystal structures. The dimer complements of AccC and AccA:AccD are shown in a darker shade. (**B**) Size exclusion chromatography revealing the most active form of ACC is a complex larger than the *E. coli* ribosome. Absorbance at 280 nm is shown in green for *E. coli* ACC purification over a Sephacryl S-500 HR column (20 MDa mass cutoff), and relative activity is shown in bar format. The red

dashed line is for the *E. coli* ribosome (2500 kDa). (**C**) SDS-PAGE of fractions from SEC purification showing the presence of the ACC proteins. The numbers for the lanes correspond to numbered fractions in the chromatogram above. The amount of material in each lane is normalized to constant absorbance at 280 nm. (**D** and **E**) Representative micrographs of helical assemblies formed in the absence (D) and in the presence (E) of substrates and $MgCl_2$, respectively. The tube highlighted by a red dashed line is longer than 0.3 μm. (**F** and **G**), Cryo-EM density maps of the narrow and the wide tubes, respectively. C5 point group symmetry of the wide tube is shown as regular pentagons and the axes of dihedral symmetries of both tubes are perpendicular to the helical axes and go through the centers of the white circles. Equivalent positions are indicated by *. (**H**) Inside the tube looking out at one of the five sets of protomers making up a ring of (G).

Production and catalytic activity of the complex

Based on reports that *E. coli* ACC complex purification from wild-type cells is notoriously difficult, we started with an overexpression plasmid containing an artificial *accA*/*accD*/*accB*/*accC*/*birA* operon, see Supplementary Materials for details and procedures. Overexpressed ACC activity is readily detectable in crude lysate and absent without induction. Classical ammonium sulfate precipitation yielded fractions with improved activity. Subsequent size exclusion chromatography (SEC) allowed purification and size characterization of the ACC complex (Fig. 1B/1C and S1A/S1B). A simple BC:BCCP:CT complex is predicted to be 270 kDa and previous report suggests a reconstituted complex is 640 kDa.[23]. Yet we isolate something much larger. Over an appropriate SEC column, ACC catalytic activity is spread between the 20 MDa exclusion limit down to the size of the *E. coli* ribosome (2,700 kDa, ~20 nm diameter) and appears to be a 1:1:1:1 ratio of AccA:AccB:AccC:AccD (Fig. 1B/1C). Our preparations have an unoptimized specific activity of 5.0 μmol/min/mg enzyme (6.8 s^{-1}). Direct comparison with previously reconstituted systems is difficult as many have subunit ratios far from equal, or only monitor half-reactions.[15,26] One study reports a specific activity at 5.6 μmol/min/mg enzyme based on 0.16 μg BC, but a limiting concentration of CT (0.32 μM BC, 0.24 μM CT, 2 μM BCCP).[23] In our preparations, the ACC complex is saturated with BCCP, as addition of extra BCCP did not increase the catalytic rate. For comparison, the yeast ACC has an activity of ~2 μmol/min/mg (8.5 s^{-1}) as a 500 kDa homodimer.[27]

Cryo-EM structure and overall atomic model.

On cryo-EM grids in the absence of substrates, the *E. coli* ACC complex formed tube-like assemblies that exhibited extremely poor order preventing structure determination (Fig. 1D). Upon incubation of the complex with ATP, acetyl-CoA, bicarbonate and Mg^{2+} for 3 minutes well-ordered tubes of various lengths were formed (Fig. 1E). Cryo-EM movies of the well-ordered tubes provided two major 2D-classes with different diameters, ~300 Å (narrow tube) or ~320 Å (wide tube) (Fig. S2). Initial helical reconstruction of both tubes yielded 3D structures with ~4 Å overall resolutions (Fig. 2F/2G). See supplemental text and Figure S3 for symmetry parameters and Table S1 for detailed data collection and refinement statistics. The subunits could be unambiguously modeled into the density. The wide tube is essentially a set of stacked rings with 10 sets of BC:BCCP:CT subunits per ring with rings offset vertically by 84 Å and rotated -27.6° with respect to the central axis (Fig. 1G and S3C). The narrow tube is helical in nature, but can also be considered as layers of rings with 10 subunit sets packed with an overlap the ends (Fig. 1F and S3D). Two sets of BC:BCCP:CT form the core linear repeating unit (Fig 1H).

Further local reconstruction yielded much improved maps for both narrow tubes (3.26 Å) and wide tubes (3.31 Å) which were used to build and refine the atomic models of ACC protomers (Fig. S4). While the overall structures of the narrow and wide tubes appear to have large deviations, the protomer cryo-EM density, ligand interactions and PPIs are essentially identical. There is modest density for CoA/acetyl-CoA in the CT and Mg^{2+}·ADP in the BC active sites reflecting the fact our structure represents an average of the catalytic states (Fig S5). Cryo-EM density for the BC domain also indicates it is in multiple conformations which are associated with multiple catalytic states (Fig. S6). Detailed descriptions of the cryo-EM density and modeling of individual subunits can be found in the supplemental text, whereas we focus on the newly discovered PPIs below.

ACC rings are generated by BC:AccD N-terminus interactions

Our structures reveal that the AccD N-terminal residues 2-23 and zinc-binding domain interacts with both the BC and BCCP (Fig. 2A-2D). Since the map was of high quality for the AccD N-terminus it reveals a network of van der Waals, hydrogen bonding and electrostatic interactions that stabilize the CT-BC-BCCP interaction (Fig. 2A). The AccD N-terminus interactions with BC and BCCP together generate 1582 $Å^2$ of buried surface area (BSA) suggesting a stable complex. In comparison, the stable BC dimer interface is 1347 $Å^2$ BSA. Even if the BCCP is displaced, the AccD:BC interactions alone generate 1145 $Å^2$ BSA. The very N-terminus of AccD binds in a previously undocumented pocket on the BC dimeric interface (Fig. 2B). The importance of the AccD:AccC interactions at the BC dimer interface for promoting tube assembly may explain the previous observations that BC mutants deficient in dimerization fail to support *E. coli* growth at physiological concentration although the BC dimerization mutants are still catalytically active.[16,28,29]

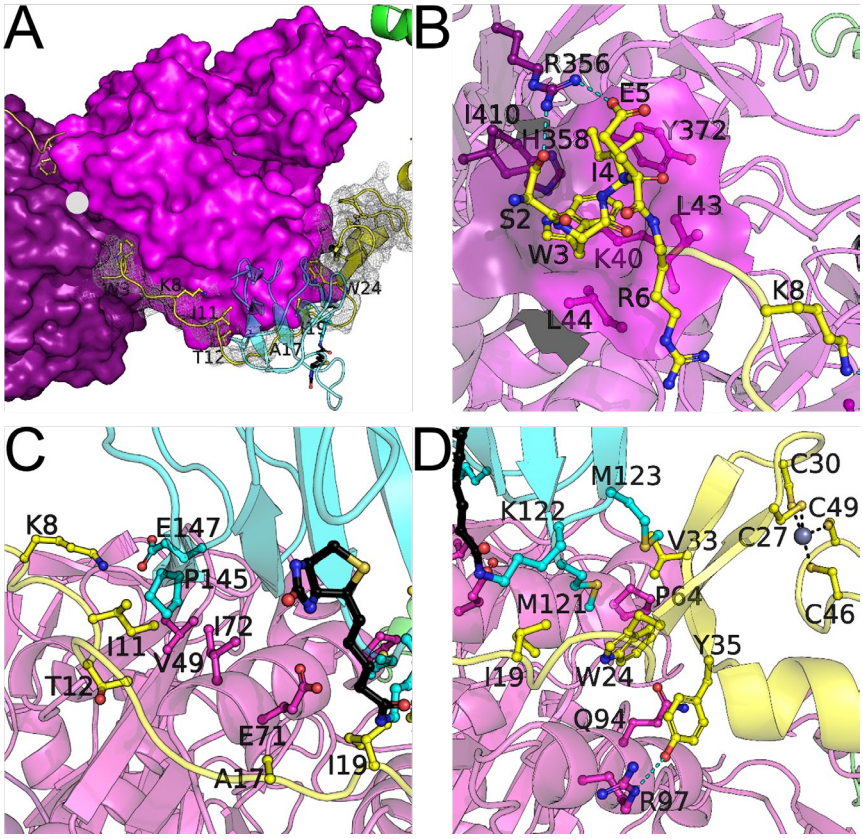

Figure 2. Detailed AccD interactions with BC and BCCP. (**A**) Overview of the AccD interactions with BC and BCCP, cryo-EM density is shown as a gray mesh and the attached biotin is shown in black. Notice the two-fold symmetry at the BC interface with the two N-termini of AccD, indicated by a ●. (**B**) The AccD Trp-3 binding pocket on the BC interface. (**C**) Hydrophobic cluster near the middle of the extended AccD N-terminus. (**D**) Hydrophobic cluster between the AccD zinc-finger domain and BC/BCCP.

Vertical interactions between rings via AccA N- and BC C-termini

The N-terminus of AccA consists of two alpha-helices (α1 residues 9-21 and α2 residues 37-57) that interact through regularly spaced hydrophobic residues in an antiparallel coiled-coils motif based on crystal structures and the AlphaFold model.[22,30] Placing the AlphaFold model in our cryo-EM density reveals the N-terminal helices make close contacts across a pseudosymmetrical plane and only partially fit the density (Fig. S7). However, due to lower resolution around the AccA N-terminal helices it is difficult to unambiguously model the interactions. In some local 3D classifications, the N-terminal helices clearly interact in a domain swapped manner, where α1 interacts with α2 from an adjacent tube layer (Fig. 3 and S8). Such interactions would act to create a stable tube, but may also play a role in catalytic regulation through long range interactions with the CT active site.

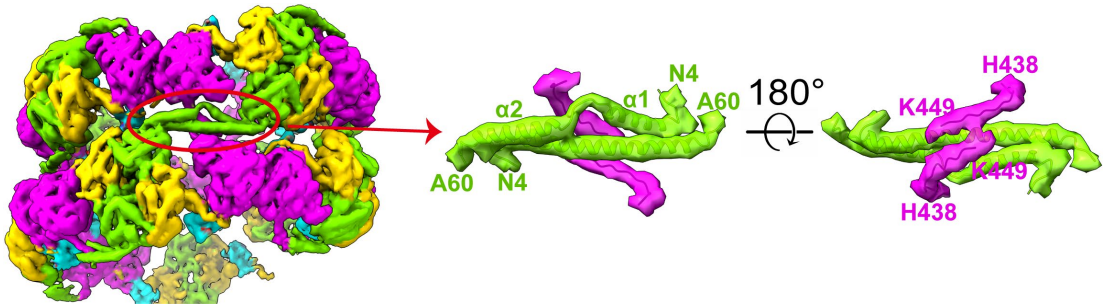

Figure 3. AccA N-terminus domain swapped model and BC interactions. One of the possible sets of asymmetric interactions at the interface between stacks of rings. This figure illustrates how the tubes can be stabilized by novel interactions likely due to the amphipathic nature of the AccA N-terminal helices. AccA interactions with the BC domain C-terminus likely alter catalysis, since the BC C-terminal helix would need to locally unfold into an extended conformation.

The N-terminal α-helices of AccA interact with the BC C-terminus, likely further stabilizing the tubes. The BC C-terminus folds into a short helix (438-444) near the ATP binding site, with the terminal residues 445-449 in most crystal structures being disordered. Based on our cryo-EM maps, the C-terminus of the BC can be modeled in an extended conformation placing hydrophobic residues Leu-444 and Leu-446 in contact with hydrophobic residues in the N-terminus of AccA (Fig. 3). Since the C-terminus of the BC is near the active site, the AccA:BC interaction can influence catalysis at the BC active site.

BCCP translocation and avoidance of diffusion away from the tube

In the two-step ACC reaction, biotinylated BCCP must cycle between BC and CT, where the biotin moiety on BCCP is carboxylated by BC, then BCCP translocates to CT where the carboxyl group is transferred from carboxybiotin to acetyl-CoA (Fig. 1A, 1F and S9).[10] There are plenty of gaps in the tube for small molecule substrates and products to flow in and out. At first glance the biotinylated BCCP appears to be well situated inside the tube fixed to the wall at a

non-catalytic site bound to the BC (previously seen in PDB 4HR7)(Fig. 4A) and AccD N-terminus (Fig. 3C/D).[31] Together these interactions generate 869 Å^2 BSA (AccD:BCCP 437 Å^2, BC:BCCP 432 Å^2), suggesting a moderately stable interaction. However, the BCCP is not at full occupancy (Fig. S4C/G), which is consistent with it in transit or bound to the catalytic active sites as our structure is a mixture of the various catalytic states. While in motion the open ends of the tube provide a chance for the BCCP to diffuse away from the compartment. This raises the question, how is the BCCP retained in the tubes?

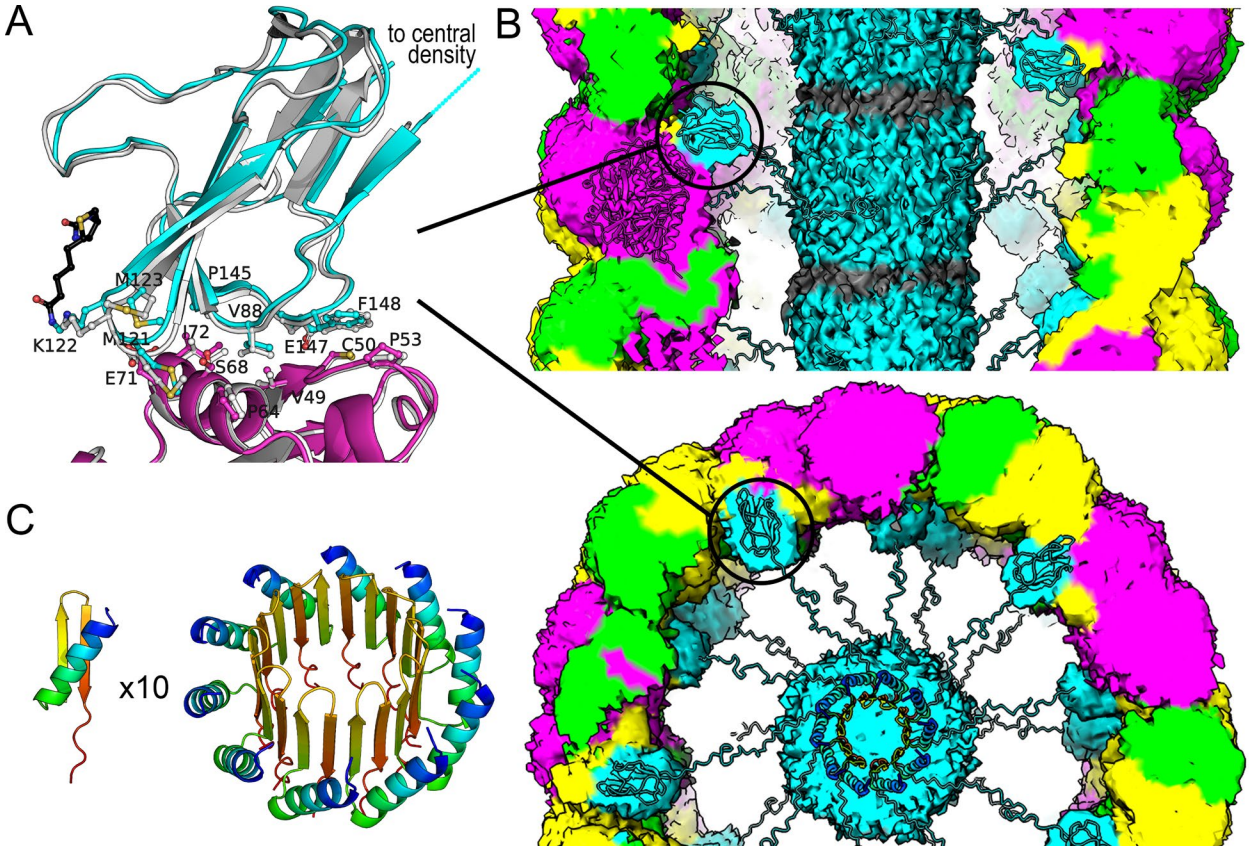

Figure 4. BCCP structure and interactions. (**A**) The interface between the BC and BCCP is shown for our cryo-EM structure, BCCP is in cyan with the attached biotin in black and BC in magenta, and the previous crystal structure in light gray. (**B**) The BCCP is near a central mass of density in our maps that can be explained by the BCCP N-terminus, which is modeled in the end on view. Linkers between the BCCP N-terminus and biotin-attachment domain are invisible in the cryo-EM maps, but shown here for scale. (**C**) An AlphaFold multimer model for 10 copies of the BCCP N-terminal 32 residues, which are predicted to fold into a β-barrel.

One answer is that the BC:BCCP interactions help to anchor the BCCPs, but that alone isn't enough. The center of the tubes has cryo-EM density that likely corresponds to the N-terminus (Fig. 4B and S10). AlphaFold2 predictions suggest that the first 30 N-terminal residues of the BCCP are folded into an α/β/β-motif (Fig. 4C). If 10 BCCP N-termini are modelled with AlphaFold Multimer, one result is a β-barrel that generates ~685 Å^2 BSA at each interface, over 6000 Å^2 total. Such a β-barrel corresponds well to the cryo-EM density in the center of the tubes (Fig. 4B). Furthermore, this arrangement keeps the biotinylated C-terminal domain of the BCCP from freely diffusing away from the tubes. While one BCCP C-terminal domain is translocating, another 10 BCCPs can hold it in position via interactions with their respective BC domains. In

the single chain dimeric eukaryotic ACCs, the BCCP is tethered to the other domains which abrogates the problem of diffusion of the BCCP away from each of the catalytic sites and creates a reaction chamber.[27,32] The length and organization of the BCCP linkers in the single chain homomeric system also creates allosteric interactions to regulate the overall catalytic activity. Here we demonstrate nature came up with a completely different architecture for ensuring the formation of a reaction chamber in the heteromeric system.

AccB N-terminus as a regulator of expression and activity in tubular filament context

It is suggested that the BCCP of the *E. coli* ACC is expressed at roughly twice the number of the catalytic AccA/AccC/AccD proteins, based on multiple lines of evidence.[10] Further evidence for double the amount of BCCP over BC and CT comes from one report, where the maximal activity of ACC required approximately twice as much BCCP as the catalytic domains.[24] In our preparations, where we expect equal numbers of the ACC subunits, the addition of extra BCCP to purified complex has no effect on catalysis and we don't see evidence for BCCP binding at either BC or CT. It may be that expression of excess BCCP in wild-type *E. coli* is used to saturate the complex at equal ratios and excess BCCP is used in other regulatory pathways. One regulatory role of AccB is upregulation of biotin biosynthesis, where the presence of apo-AccB, alleviates biotin synthesis repression. Another regulatory role is sequestration of AccB by GlnB, linking fatty acid biosynthesis and nitrogen regulation.[8,9]

The N-terminus of AccB alone (residues 1-68) can negatively regulate expression of the *accB*/*accC* operon in *E. coli*, yet our structure suggests a biophysical role for the N-terminus.[5] Early studies established in vitro *E. coli* ACC activity were dependent on high protein concentration.[33,34] This suggests growth or cell-cycle dependent concentration changes of ACC in vivo can regulate activity. Measurements of *accB* mRNA and AccB protein levels of *E. coli* during growth indicate that as cell density increases and cells enter stationary phase, mRNA levels decrease but protein levels remain constant.[35] The decrease in ATP and acetyl-CoA concentrations that accompanies transition to stationary phase could drive an ACC order to disorder transition that we see in cryo-EM images in the absence of substrates (Fig. 1D and 1E). Such a transition would allow greater access to the BCCP N-terminus for transcriptional repression.

Relevance of *E. coli* ACC structure to other heteromeric systems

A phylogenetic tree generated from concatenation of AccC/AccB/AccD/AccA from various organisms reveals two major clades (Fig. S11 and S12). The *E. coli* ACC is almost identical to species from pathogenic genus like *Brucella*, *Acinetobacter*, *Bordetella*, *Pseudomonas*, *Hemophilus*, *Vibrio*, *Yersinia*, *Salmonella*, *Klebsiella* and *Enterobacter*, with identities between 60-99%. Even cyanobacteria and plant plastidial ACCs are closely related to the *E. coli* ACC at greater than 49% and 45%, respectively. ACCs from *E. coli* and Gram-positive organisms share significant identity with an average around 45%. Most importantly, the PPI residues of the *E. coli* tubular structures are conserved in other organisms, even if the interactions between the rings are not, Supplementary Text and Figure S12.

Higher-order polymer formation by ACCs

We have revealed that the heteromeric *E. coli* ACC should be added to the growing list of enzymes that form filaments.[36] Human ACC contains all the domains on a single polypeptide, which forms a homodimer. The homodimer polymerizes into a filament in the presence of citrate or isocitrate to form an active complex. Another acyl-CoA carboxylase, 3-methylcrotonyl-CoA

carboxylase from *Leishmania tarentola*, was also recently shown to form a filament in an inactive state.[37] The observation of diverse acyl-CoA carboxylase oligomeric states suggests that filament formation is a broader feature of carboxyltransferase regulation across domains of life. Our demonstration that heteromeric complexes can be purified and structurally characterized, sets the stage to further examine the role of tubular filament formation and regulation for the heteromeric ACC family of enzymes.

Conclusions

Our *E. coli* heteromeric ACC cryo-EM structures also raises many questions. For example, does the tube support crosstalk between the CT and BC active sites, which is suggested form kinetics experiments? Another question is, do *E. coli* ACC allosteric regulators like fatty acid bearing acyl carrier protein or GlnB, induce a disordered state as seen in the cryo-EM images without substrates? Experiments that allow examination of each tube catalytic state and dynamics are needed to provide that deeper level of understanding. It's likely that cryo-EM tomography and the use of substrate analogs that prevent turnover will help achieve that deeper level of knowledge. Nevertheless, our cryo-EM structures provide a scaffold for modeling and testing allosteric mechanisms and address several lingering questions. The N-termini of AccA/B/D are functional rather than vestigial and play key roles in tube formation for setting up the catalytic active sites in close proximity. The AccD zinc-finger domain is buried in the complex masking a putative role in translational repression and suggest the zinc-finger domain is primarily involved in PPIs. Bioinformatics along with our structures show the PPIs are likely conserved from prokaryotes to plants and set the stage to model plant ACC regulation for biofuel engineering. Finally, based on the uncovered PPIs our structures can be used to launch antibiotic drug discovery programs to combat the growing problem of antibiotic resistance.

References and Notes

1 Tong, L. Structure and function of biotin-dependent carboxylases. *Cell Mol Life Sci* **70**, 863-891, doi:10.1007/s00018-012-1096-0 (2013).

2 Heath, R. J. & Rock, C. O. Regulation of Fatty Acid Elongation and Initiation by Acyl-Acyl Carrier Protein inEscherichia coli. *Journal of Biological Chemistry* **271**, 1833-1836, doi:10.1074/jbc.271.4.1833 (1996).

3 Evans, A., Ribble, W., Schexnaydre, E. & Waldrop, G. L. Acetyl-CoA carboxylase from Escherichia coli exhibits a pronounced hysteresis when inhibited by palmitoyl-acyl carrier protein. *Archives of biochemistry and biophysics* **636**, 100-109, doi:10.1016/j.abb.2017.10.016 (2017).

4 Davis, M. S. & Cronan, J. E., Jr. Inhibition of Escherichia coli acetyl coenzyme A carboxylase by acyl-acyl carrier protein. *Journal of bacteriology* **183**, 1499-1503, doi:10.1128/JB.183.4.1499-1503.2001 (2001).

5 James, E. S. & Cronan, J. E. Expression of two Escherichia coli acetyl-CoA carboxylase subunits is autoregulated. *The Journal of biological chemistry* **279**, 2520-2527, doi:10.1074/jbc.M311584200 (2004).

6 Meades, G., Jr., Benson, B. K., Grove, A. & Waldrop, G. L. A tale of two functions: enzymatic activity and translational repression by carboxyltransferase. *Nucleic acids research* **38**, 1217-1227, doi:10.1093/nar/gkp1079 (2010).

7 Rodrigues, T. E. *et al.* Fatty acid biosynthesis is enhanced in Escherichia coli strains with deletion in genes encoding the PII signaling proteins. *Arch Microbiol* **201**, 209-214, doi:10.1007/s00203-018-1603-2 (2019).

8 Rodrigues, T. E. *et al.* Search for novel targets of the PII signal transduction protein in Bacteria identifies the BCCP component of acetyl-CoA carboxylase as a PII binding partner. *Molecular microbiology* **91**, 751-761, doi:10.1111/mmi.12493 (2014).

9 Gerhardt, E. C. *et al.* The bacterial signal transduction protein GlnB regulates the committed step in fatty acid biosynthesis by acting as a dissociable regulatory subunit of acetyl-CoA carboxylase. *Molecular microbiology* **95**, 1025-1035, doi:10.1111/mmi.12912 (2015).

10 Cronan, J. E. The Classical, Yet Controversial, First Enzyme of Lipid Synthesis: Escherichia coli Acetyl-CoA Carboxylase. *Microbiology and Molecular Biology Reviews*, doi:10.1128/mmbr.00032-21 (2021).

11 Salie, M. J. & Thelen, J. J. Regulation and structure of the heteromeric acetyl-CoA carboxylase. *Biochimica et biophysica acta* **1861**, 1207-1213, doi:10.1016/j.bbalip.2016.04.004 (2016).

12 Radka, C. D. & Rock, C. O. Mining Fatty Acid Biosynthesis for New Antimicrobials. *Annual review of microbiology* **76**, 281-304, doi:10.1146/annurev-micro-041320-110408 (2022).

13 Fall, R. R. Stabilization of an acetyl-coenzyme a carboxylase complex from Pseudomonas citronellolis. *Biochimica et Biophysica Acta (BBA) - Lipids and Lipid Metabolism* **450**, 475-480, doi:10.1016/0005-2760(76)90022-9 (1976).

14 Lane, M. D., Moss, J. & Polakis, S. E. *Current Topics in Cellular Regulation* 139-195 (1974).

15 Guchhait, R. B. *et al.* Acetyl Coenzyme A Carboxylase System of Escherichia coli. *Journal of Biological Chemistry* **249**, 6633-6645, doi:10.1016/s0021-9258(19)42203-5 (1974).

16 Shen, Y., Chou, C. Y., Chang, G. G. & Tong, L. Is dimerization required for the catalytic activity of bacterial biotin carboxylase? *Mol Cell* **22**, 807-818, doi:10.1016/j.molcel.2006.04.026 (2006).

17 Mochalkin, I. *et al.* Structural evidence for substrate-induced synergism and half-sites reactivity in biotin carboxylase. *Protein science : a publication of the Protein Society* **17**, 1706-1718, doi:10.1110/ps.035584.108 (2008).

18 Janiyani, K., Bordelon, T., Waldrop, G. L. & Cronan, J. E., Jr. Function of Escherichia coli biotin carboxylase requires catalytic activity of both subunits of the homodimer. *The Journal of biological chemistry* **276**, 29864-29870, doi:10.1074/jbc.M104102200 (2001).

19 Blanchard, C. Z., Lee, Y. M., Frantom, P. A. & Waldrop, G. L. Mutations at four active site residues of biotin carboxylase abolish substrate-induced synergism by biotin. *Biochemistry* **38**, 3393-3400, doi:10.1021/bi982660a (1999).

20 de Queiroz, M. S. & Waldrop, G. L. Modeling and numerical simulation of biotin carboxylase kinetics: implications for half-sites reactivity. *J Theor Biol* **246**, 167-175, doi:10.1016/j.jtbi.2006.12.025 (2007).

21 Athappilly, F. K. & Hendrickson, W. A. Structure of the biotinyl domain of acetyl-coenzyme A carboxylase determined by MAD phasing. *Structure* **3**, 1407-1419, doi:10.1016/s0969-2126(01)00277-5 (1995).

22 Bilder, P. *et al.* The structure of the carboxyltransferase component of acetyl-coA carboxylase reveals a zinc-binding motif unique to the bacterial enzyme. *Biochemistry* **45**, 1712-1722, doi:10.1021/bi0520479 (2006).

23 Broussard, T. C., Price, A. E., Laborde, S. M. & Waldrop, G. L. Complex formation and regulation of Escherichia coli acetyl-CoA carboxylase. *Biochemistry* **52**, 3346-3357, doi:10.1021/bi4000707 (2013).

24 Soriano, A. *et al.* Escherichia coli acetyl-coenzyme A carboxylase: characterization and development of a high-throughput assay. *Analytical biochemistry* **349**, 268-276, doi:10.1016/j.ab.2005.10.044 (2006).

25 Davis, M. S., Solbiati, J. & Cronan, J. E., Jr. Overproduction of acetyl-CoA carboxylase activity increases the rate of fatty acid biosynthesis in Escherichia coli. *The Journal of biological chemistry* **275**, 28593-28598, doi:10.1074/jbc.M004756200 (2000).

26 Guchhait, R. B., Moss, J., Sokolski, W. & Lane, M. D. The carboxyl transferase component of acetyl CoA carboxylase: structural evidence for intersubunit translocation of the biotin prosthetic group. *Proceedings of the National Academy of Sciences of the United States of America* **68**, 653-657, doi:10.1073/pnas.68.3.653 (1971).

27 Wei, J. & Tong, L. Crystal structure of the 500-kDa yeast acetyl-CoA carboxylase holoenzyme dimer. *Nature* **526**, 723-727, doi:10.1038/nature15375 (2015).

28 Smith, A. C. & Cronan, J. E. Dimerization of the bacterial biotin carboxylase subunit is required for acetyl coenzyme A carboxylase activity in vivo. *Journal of bacteriology* **194**, 72-78, doi:10.1128/JB.06309-11 (2012).

29 Chou, C. Y. & Tong, L. Structural and biochemical studies on the regulation of biotin carboxylase by substrate inhibition and dimerization. *The Journal of biological chemistry* **286**, 24417-24425, doi:10.1074/jbc.M111.220517 (2011).

30 Jumper, J. *et al.* Highly accurate protein structure prediction with AlphaFold. *Nature* **596**, 583-589, doi:10.1038/s41586-021-03819-2 (2021).

31 Broussard, T. C. *et al.* The three-dimensional structure of the biotin carboxylase-biotin carboxyl carrier protein complex of E. coli acetyl-CoA carboxylase. *Structure* **21**, 650-657, doi:10.1016/j.str.2013.02.001 (2013).

32 Hunkeler, M. *et al.* Structural basis for regulation of human acetyl-CoA carboxylase. *Nature* **558**, 470-474, doi:10.1038/s41586-018-0201-4 (2018).

33 Alberts, A. W. & Vagelos, P. R. Acetyl CoA carboxylase. I. Requirement for two protein fractions. *Proceedings of the National Academy of Sciences of the United States of America* **59**, 561-568, doi:10.1073/pnas.59.2.561 (1968).

34 Cronan, J. E. & Waldrop, G. L. Multi-subunit acetyl-CoA carboxylases. *Progress in Lipid Research* **41**, 407-435, doi:10.1016/s0163-7827(02)00007-3 (2002).

35 Li, S. J. & Cronan, J. E., Jr. Growth rate regulation of Escherichia coli acetyl coenzyme A carboxylase, which catalyzes the first committed step of lipid biosynthesis. *Journal of bacteriology* **175**, 332-340, doi:10.1128/jb.175.2.332-340.1993 (1993).

36 Park, C. K. & Horton, N. C. Structures, functions, and mechanisms of filament forming enzymes: a renaissance of enzyme filamentation. *Biophys Rev* **11**, 927-994, doi:10.1007/s12551-019-00602-6 (2019).

37 Hu, J. J. *et al.* Discovery, structure, and function of filamentous 3-methylcrotonyl-CoA carboxylase. *Structure* **31**, 100-110 e104, doi:10.1016/j.str.2022.11.015 (2023).

Acknowledgments:

Funding:

Purdue Institute for Drug Discovery (JRL)

National Institutes of Health grant R01 GM140290 (JL, WJ)

Author contributions:

Conceptualization: JRL

Methodology: JRL, WJ

Investigation: XX, AS, TJB

Visualization: XX, AS, JRL

Funding acquisition: JRL, WJ

Project administration: JRL

Supervision: JRL, WJ

Writing – original draft: JRL, XX

Writing – review & editing: JRL, XX, AS, TJB, WJ

Competing interests: Authors declare that they have no competing interests.

Data and materials availability:

The cryo-EM maps and coordinates for the *E. coli* ACC structures have been deposited in the Protein Data Bank and Electron Microscopy Data Bank. The depositions can be accessed with the following codes, PDB 8UW5/EMD 42638 for the narrow tube ring stack, PDB 8UWO/EMD 42679 for the wide tube ring stack, PDB 8UZ2/EMD 42831 for the narrow tube protomer, and PDB 8UXZ/EMD 42790 for the wide tube protomer.

Supplementary Materials

Materials and Methods

Supplementary Text

Figs. S1 to S12

Table S1